

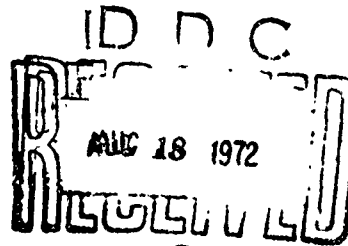
AD 746699

AFOSR Scientific Report  
AFOSR-TR-72-1107

# Instabilities of a Spatial System of Articulated Pipes Conveying Fluid

by

**Michael P. Bohn  
and  
George Herrmann**



Air Force Office of Scientific Research  
Grant AFOSR 70-1905

**SUDAM Report No. 72-8**

JUNE 1972

Approved for Public Release; Distribution Unlimited

Reproduced by  
**NATIONAL TECHNICAL  
INFORMATION SERVICE**  
U.S. Department of Commerce  
Washington, D.C. 20540

DEPARTMENT  
OF  
**APPLIED  
MECHANICS**



**STANFORD  
UNIVERSITY**

STANFORD,  
CALIFORNIA  
94305

ACCESSION for	
NTIS	Units Section <input checked="" type="checkbox"/>
DDI	Doc. Section <input type="checkbox"/>
U.S. DTIC	<input type="checkbox"/>
BY	
DIS. SECTION/AVAILABILITY CODES	
Dist.	Special
A	

Qualified requestors may obtain additional copies from the Defense Documentation Center, all others should apply to the National Technical Information Service.

Reproduction, translation, publication, use and disposal in whole or in part by or for the United States Government is permitted.

UNCLASSIFIED

Security Classification

DOCUMENT CONTROL DATA - R & D		
<i>(Security classification of title, body of abstract and indexing annotation must be entered when the overall report is classified)</i>		
1. ORIGINATING ACTIVITY (Corporate author) STANFORD UNIVERSITY DEPARTMENT OF APPLIED MECHANICS STANFORD, CALIFORNIA 94305		2a. REPORT SECURITY CLASSIFICATION UNCLASSIFIED
		2b. GROUP
3. REPORT TITLE  INSTABILITIES OF A SPATIAL SYSTEM OF ARTICULATED PIPES CONVEYING FLUID		
4. DESCRIPTIVE NOTES (Type of report and inclusive dates) Scientific Interim		
5. AUTHOR(S) (First name, middle initial, last name) MICHAEL P BOHN GEORGE HERRMANN		
6. REPORT DATE June 1972	7a. TOTAL NO. OF PAGES 32	7b. NO. OF REFS 5
8a. CONTRACT OR GRANT NO AFOSR-70-1905	8b. ORIGINATOR'S REPORT NUMBER(S) SUDAM Report No. 72-8	
a. PROJECT NO. 9782-01		
c. 61102F	9b. OTHER REPORT NO(S) (Any other numbers that may be assigned this report)	
d. 681307	AFOSR-TR-72-1107	
10. DISTRIBUTION STATEMENT  Approved for public release; distribution unlimited.		
11. SUPPLEMENTARY NOTES  TECH, OTHER	12. SPONSORING MILITARY ACTIVITY AF Office of Scientific Research (NAM) 1400 Wilson Boulevard Arlington, Virginia 22209	
13. ABSTRACT A spatial system of two articulated pipes conveying fluid is examined analytically and experimentally. As the flowrate is increased, stable equilibrium may be lost by either divergence (static buckling) or by flutter (oscillations with increasing amplitude), depending upon the value of an angle $\beta$ which measures the "out-of-planeness" of the system. It is found that in the range $0 < \beta < 90^\circ$ there exists a transition value $\beta^*$ below which stability is lost by flutter and above which stability is lost by divergence.		

DD FORM 1473  
1 NOV 68

UNCLASSIFIED

Security Classification

UNCLASSIFIED

Security Classification

14 KEY WORDS	LINK A		LINK B		LINK C	
	RDL	WT	ROLE	WT	ROLE	WT
STABILITY						
FLOW THROUGH PIPES						
DIVERGENCE						
FLUTTER						

UNCLASSIFIED

Security Classification

11

INSTABILITIES OF A SPATIAL SYSTEM  
OF  
ARTICULATED PIPES CONVEYING FLUID

by  
MICHAEL P. BOHN  
STANFORD UNIVERSITY  
and  
GEORGE HERRMANN  
STANFORD UNIVERSITY

This work was supported in part by AFOSR Grant 70-1905 and NASA  
Grant NGL 05-020-397 to Stanford University.

Approved for public release;  
distribution is unlimited.

## 1. Introduction

The last decade has witnessed a great surge of academic interest in the dynamic behavior and stability of mechanical systems with follower (circulatory) forces, i.e. forces which are not derivable from a potential, as evidenced by references [1] to [4]. It is a peculiar common feature of much published analytical work on this subject that the possible physical origin of such forces is not mentioned. The follower forces are introduced into the analysis either through a sketch, with forces being merely indicated by arrows, or through a specified functional dependence of the forces on generalized coordinates. Thus the purportedly physical problem is reduced immediately to mathematical analysis and the relationship to mechanics becomes most tenuous. The motivation for much of this type of work appears to have been sheer curiosity in determining the sometimes unexpected behavior of an imagined system, rather than a modeling and an explanation of observed phenomena.

One of the possible ways to realize follower forces is by conveying fluid through articulated or continuously flexible pipes. The pioneering work in this class of mechanical systems with follower forces was carried out by Benjamin [5]. He examined analytically and experimentally a system with two degrees of freedom consisting of two articulated pipe segments, constrained to motion in a plane like a double pendulum, and conveying fluid. It was found that, depending upon the values of relevant parameters, the system could lose stability by static buckling (passage to an adjacent equilibrium position,

divergence) or by dynamic instability (oscillations with increasing amplitude, flutter). Several other workers considered various aspects of the dynamic behavior of continuous pipes conveying fluid, as mentioned in [4]. However, the transition from one type of loss of stability to another was not investigated systematically and quantitatively.

The purpose of the present investigation is to study the various modes of instability of a mechanical system whose non-conservative character arises in a completely natural manner, and to verify that the transitions between the instability modes (as predicted by the linearized dynamic equations of motion) are indeed experimentally obtainable. To this end, a spatial system of articulated pipes is considered. This system is a generalization of the plane one discussed by Benjamin. Instability either by divergence or by flutter is possible, but due to the presence of an additional parameter which measures the "out-of-planeness" of the system, a wider variety of types of behavior is possible.

The feature of the spatial system chosen is that one can experimentally observe the various modes of instability by simply varying the "out-of-planeness" of the system. By contrast, in Benjamin's work, it was necessary to use sets of pipes of different mass densities to observe different types of instability.

## 2. The System

We consider here a generalization of Benjamin's system, allowing the pipe segments to oscillate in two different planes. The system consists of two straight pipe segments, with the upper segment pinned

at its upper end  $O$  in such a manner that it is constrained to move in a single vertical plane, the  $x$ - $y$  plane as shown in Fig. 1. The lower segment is pinned to the upper one at  $P$  such that an angle  $\beta$  is formed between the  $z$ -axis and the normal to the plane of motion of the lower segment (i.e. the pin axis  $\underline{e}_2$ ). Thus for  $\beta = 0$  the motion of the two segments occurs in the same plane, while for  $\beta = 90^\circ$  the planes of motion are normal to one another.

An incompressible fluid enters the upper segment at  $O$  and is discharged at the free end of the lower segment. It will be assumed that the rate of discharge of the fluid is constant, i.e. that the fluid velocity is constant. At the joints, linear restoring springs and linear viscous damping are introduced.

### 3. The Equations of Motion

Following Benjamin [5], the equations of motion of the system with two degrees of freedom under consideration may be derived from the Lagrangian form

$$\frac{d}{dt} \left( \frac{\partial L}{\partial \dot{q}_i} \right) - \frac{\partial L}{\partial q_i} + \frac{\partial D}{\partial \dot{q}_i} = - \rho V A (V \underline{e}_t + \underline{R}) \cdot \frac{\partial \underline{R}}{\partial q_i} ; \quad i=1,2$$

where  $q_i$  are the angles shown in Fig. 1 and  $\dot{q}_i$  are the corresponding angular velocities and

$\underline{R}$  = Position vector of free end (see Fig. 1)

$\underline{e}_t$  = Unit vector tangent to the free end

$V$  = Fluid flowrate relative to the pipes

$$L = T_1 + T_2 - V_1 - V_2$$

$T_1$  = Kinetic energy of the pipes alone

$T_2$  = Kinetic energy of the fluid instantaneously within the pipes

$V_1$  = Potential energy of the pipes alone

$V_2$  = Potential energy of the fluid instantaneously within the pipes

$A$  = Inside cross-sectional area of the pipes, assumed the same  
for both segments

$\rho$  = Mass density of the fluid

$D$  = Rayleigh's Dissipation function.

In the following, the segments are assumed to be axisymmetric about the center line of the flow channel. The derivation of the equations and their linearization about the position of equilibrium  $q_1 = q_2 = 0$  is straightforward. The potential and kinetic energies are given by

$$V_1 = - M_A g a \cos q_1 - 0.5(K_1 q_1^2 + K_2 q_2^2)$$

$$- M_B g [(L_A + b \cos q_2) \cos q_1 - b C\beta \sin q_1 \sin q_2]$$

$$V_2 = - \rho A L_A g (0.5 L_A \cos q_1)$$

$$- \rho A L_B g [(L_A + 0.5 L_B \cos q_2) \cos q_1 - 0.5 L_B C\beta \sin q_1 \sin q_2]$$

$$2T_1 = I_{zz}^A \dot{q}_1^2 + M_B \left\{ [S\beta \dot{q}_1 (L_A + b \cos q_2)]^2 \right.$$

$$\left. + [b \dot{q}_2 + C\beta \dot{q}_1 (b + L_A \cos q_2)]^2 + [L_A \dot{q}_1 C\beta \sin q_2]^2 \right\}$$

$$+ \bar{I}_{11}^B (\dot{q}_1 S\beta \cos q_2)^2 + (\dot{q}_2 + C\beta \dot{q}_1)^2 \bar{I}_{22}^B + (\dot{q}_1 S\beta \sin q_2)^2 \bar{I}_{33}^B$$

$$\begin{aligned}
 2T_2 = \rho A \{ & V^2 L_A + L_A^3 \dot{q}_1^2 / 3 + (\dot{q}_2 + C\beta \dot{q}_1)^2 L_B^3 / 3 \\
 & + L_B^2 (\dot{q}_2 + C\beta \dot{q}_1) (C\beta L_A \dot{q}_1 \cos q_2) \\
 & + L_B (\dot{q}_1 L_A C\beta \cos q_2)^2 + L_B (L_A \dot{q}_1 S\beta)^2 \\
 & + I_A L_B^2 \cos^2 q_2 (\dot{q}_1 S\beta)^2 + L_B^3 (\dot{q}_1 S\beta \cos q_2)^2 / 3 \\
 & + L_B V^2 + 2V L_A L_B \dot{q}_1 C\beta \sin q_2 + L_B (L_A \dot{q}_1 C\beta \sin q_2)^2 \}
 \end{aligned}$$

where

$I_{zz}^A$  = Moment of inertia of upper segment with respect to  $z$  axis through point 0 (see Fig. 1)

$\bar{I}_{11}^B, \bar{I}_{22}^B, \bar{I}_{33}^B$  = Principal moments of inertia for the mass center of the lower segment with respect to  $\underline{e}_1, \underline{e}_2$  and  $\underline{e}_3$  axes

$M_A, M_B$  = Masses of upper and lower segments

$L_A, L_B$  = Lengths of upper and lower segments

$a$  = Distance from mass center of upper segment to point 0

$b$  = Distance from mass center of lower segment to point P

$g$  = Acceleration of gravity

$C\beta = \cos(\beta)$

$S\beta = \sin(\beta)$

$K_1, K_2$  = Linear spring constants at upper and lower joints, respectively

$R_1, R_2$  = Linear viscous damping constants at upper and lower joints, respectively

The equations of motion are then obtained as

$$\begin{aligned}
 & \ddot{q}_1 [\bar{I}_{zz}^A + \bar{I}_{11}^B + M_B b^2 + M_B L_A^2 + 2M_B b L_A \\
 & + \rho A (L_A^3 + L_B^3)/3 + \rho A L_A L_B (L_A + L_B)] \\
 & + \ddot{q}_2 [C_B (\bar{I}_{11}^B + M_B b^2 + M_B L_A b + \rho A L_B^3/3 + \rho A L_A L_B^2/2)] \\
 & + \dot{q}_1 [\rho A V (L_A + L_B)^2 + R_1] + \dot{q}_2 [C_B \rho A V (2L_A L_B + L_B^2)] \\
 & + q_1 [M_A g a + M_B g (L_A + b) + 0.5 \rho A g (L_A + L_B)^2 + K_1] \\
 & + q_2 [C_B (0.5 \rho A g L_B^2 + M_B g b + \rho A V^2 L_A)] = 0 \tag{1}
 \end{aligned}$$

and

$$\begin{aligned}
 & \ddot{q}_1 [C_B (\bar{I}_{11}^B + M_B b^2 + M_B b L_A + \rho A L_B^3/3 + \rho A L_A L_B^2/2)] \\
 & + \ddot{q}_2 [\bar{I}_{11}^B + M_B b^2 + \rho A L_B^3/3] \\
 & + \dot{q}_1 [C_B \rho A V L_B^2] + \dot{q}_2 [\rho A V L_B^2 + R_2] \\
 & + q_1 [C_B (0.5 \rho A g L_B^2 + M_B g b)] \\
 & + q_2 [0.5 \rho A g L_B^2 + M_B g b + K_2] = C \tag{2}
 \end{aligned}$$

In the first part of the paper attention is restricted to the idealized case in which the upper and lower segments are straight pipes of uniform cross-section and no spring or damping forces act at the joints. For this case:

$$K_1 = K_2 = 0$$

$$R_1 = R_2 = 0$$

$$I_{zz}^A = M_A L_A^2 / 3$$

$$I_{11}^B = M_B L_B^2 / 12$$

$$a = L_A / 2$$

$$b = L_B / 2$$

Following Benjamin [5], we assume the pipes to have the same mass density per unit length,  $\eta$ . Then, introducing the following non-dimensional parameters

$$\left. \begin{aligned} \alpha &= L_A / L_B \\ \gamma &= 3 \rho A / (\eta + \rho A) \\ U &= \gamma V / \sqrt{1.5 g L_B} \\ t^* &= \sqrt{1.5 g / L_B} t \end{aligned} \right\} \quad (3)$$

the equations of motion are transformed to the non-dimensional form

$$\begin{aligned} & \begin{bmatrix} (\alpha + 1)^3 & 0.5 C\beta(2 + 3\alpha) \\ 0.5 C\beta(2 + 3\alpha) & 1 \end{bmatrix} \begin{bmatrix} q_1'' \\ q_2'' \end{bmatrix} \\ + & \begin{bmatrix} (\alpha + 1)^2 U & C\beta(1 + 2\alpha) U \\ C\beta U & U \end{bmatrix} \begin{bmatrix} q_1' \\ q_2' \end{bmatrix} \\ + & \begin{bmatrix} (\alpha + 1)^2 & C\beta(1 + \alpha U^2 / \gamma) \\ C\beta & 1 \end{bmatrix} \begin{bmatrix} q_1 \\ q_2 \end{bmatrix} = 0 \end{aligned} \quad (4)$$

where ( )' denotes  $d/dt^*$ .

#### 4. Stability Analysis

We shall examine the nature of the solutions of the form

$$q_i = Q_i e^{\lambda t}, \quad i=1,2 \quad (5)$$

which, upon substitution into the equations of motion, leads to the characteristic equation

$$A_4 \lambda^4 + A_3 \lambda^3 + A_2 \lambda^2 + A_1 \lambda + A_0 = 0 \quad (6)$$

where

$$\left. \begin{aligned} A_4 &= \alpha^3 + \alpha^2(3 - 2.25 C\beta^2) + (1 + 3\alpha) S\beta^2 \\ A_3 &= U[\alpha^3 + \alpha^2(4 - 3C\beta^2) + 5\alpha S\beta^2 + 2S\beta^2] \\ A_2 &= (\alpha + 1)^3 + (\alpha + 1)^2(1 + U^2) \\ &\quad - C\beta^2[(1 + 1.5\alpha)(2 + \alpha U^2/\gamma) + (1 + 2\alpha)U^2] \\ A_1 &= 2(\alpha + 1)^2 U - C\beta^2[2(\alpha + 1)U + \alpha U^3/\gamma] \\ A_0 &= (\alpha + 1)^2 - C\beta^2[1 + \alpha U^2/\gamma] \end{aligned} \right\} (7)$$

The position of equilibrium  $q_1 = q_2 = 0$  is said to be stable provided all the characteristic exponents have negative real parts. The well-known Routh-Hurwitz [3] criterion, applied to the fourth order polynomial at hand, assures stability if

$$\left\{ \begin{aligned} A_i &> 0 \quad i=0,1,\dots,4 \\ X &\equiv A_1 A_2 A_3 - A_0 A_3^2 - A_1^2 A_4 > 0 \end{aligned} \right. \quad (8)$$

If any of the above conditions are violated, the system will be unstable.

A simplification is possible since both  $A_4$  and  $A_3$  are always positive. For small  $U$ , all  $A_i$  are positive. Suppose as  $U$  increases  $A_1$  vanishes, while the remaining  $A_i$  are positive. Then  $X$  must be negative, and hence  $X$  vanishes before  $A_1$ . The same applies to  $A_2$ . Thus the six requirements for stability (8) may be replaced by just two conditions

$$\begin{cases} A_0 > 0 \\ X > 0 \end{cases} \quad (9)$$

Loss of stability can thus occur in two different ways. If  $A_0 = 0$ , there will be a root  $\lambda = 0$  which corresponds to an adjacent equilibrium position, i.e. to static Euler buckling (divergence). By contrast when  $X < 0$ , the characteristic exponents  $\lambda$  will be complex with positive real parts, and stability will be lost by oscillations with increasing amplitude (flutter). Written out we have

$$\begin{aligned} X = U^6 & \left\{ [ -(\alpha/\gamma)(\alpha + 1)^2(\alpha^3 + 4\alpha^2 + 5\alpha + 2) ] C\beta^2 \right. \\ & + C\beta^4 \left[ (\alpha/\gamma)(\alpha + 1)^2(5\alpha^2 + 10\alpha + 4) \right. \\ & + (\alpha/\gamma)^2(\alpha + 1)^2 \left( \frac{3}{2}\alpha^2 + 3\alpha + 1 \right) \left. \right] \\ & + C\beta^6 \left[ -(\alpha/\gamma)(6\alpha^3 + 11\alpha^2 + 9\alpha + 2) \right. \\ & - (\alpha/\gamma)^2 \left( \frac{1}{4} \right) (18\alpha^3 + 33\alpha^2 + 27\alpha + 4) \left. \right] \left. \right\} \\ & + U^4 \left\{ 2[(\alpha + 1)^7 + (\alpha + 1)^6] \right. \end{aligned}$$

$$\begin{aligned}
 & + C\beta^2(\alpha + 1)^4 [-2(6\alpha^2 + 13\alpha + 6) - (\alpha/\gamma)(3\alpha^2 + 4\alpha)] \\
 & + C\beta^4(\alpha + 1)^2 [22\alpha^3 + 56\alpha^2 + 46\alpha + 12 + (\alpha/\gamma)(9\alpha^3 + 11\alpha^2 + 4\alpha)] \\
 & + C\beta^6(\alpha + 1)^2 [-2(2\alpha + 1)(2 + 3\alpha)] \} \\
 & + U^2 \{ [\alpha^2(\alpha + 1)^6] + C\beta^2[(\alpha + 1)^4(2\alpha^2 - 2\alpha^3)] \\
 & + C\beta^4[-(\alpha + 1)^3(3\alpha^2 + 3\alpha^3)] \} \tag{10}
 \end{aligned}$$

If the flowrate  $U$  is very small, the position of equilibrium  $q_1 = q_2 = 0$  is clearly stable. As the flowrate is slowly increased, Benjamin [5] has shown that in his plane case ( $\beta = 0$ ) instability occurs first by buckling if  $\gamma > 0.5$  and by flutter if  $\gamma < 0.5$ . It is found that in the present spatial case ( $\beta \neq 0$ ) the value  $\gamma = 0.5$  still separates the two different modes of loss of stability.

#### The Case $\gamma > 0.5$

It is proposed to show that if  $\gamma > 0.5$ , loss of stability can occur only by buckling, as the flowrate is increased, no matter what the value of  $\beta$ . To accomplish this it must be shown that  $A_0$  becomes zero before  $X$  does, as the flowrate is increased.

The flowrate for vanishing  $A_0$ , denoted  $U_B$ , is obtained from (7) as

$$U_B^2 = (\gamma/\alpha)[(\alpha + 1)^2/C\beta^2 - 1] \tag{11}$$

As  $\beta$  increases,  $U_B$  increases and at  $\beta = 90^\circ$ , no finite value of  $U$  can cause instability.

On substitution of  $U_B$  into the expression for  $X$  given by (10),

a polynomial in powers of  $\alpha$  is obtained of the form

$$X = \left[ U_B^2 / (\alpha C\beta^2) \right] \sum_{n=1}^9 \alpha^n [B_{n1} \gamma + B_{n2}] \quad (12)$$

where the  $B_{ij}$  are polynomials in  $C\beta$ . The coefficient of  $\alpha^9$  is given by

$$\gamma - 0.5 C\beta^2$$

and thus it is seen that a necessary condition for  $X$  to be positive for all  $\alpha$  and  $\beta$  is that  $\gamma > 0.5$ . Further, it is readily shown that the  $B_{n1}$  terms are all non-negative in the remaining coefficients. Hence the value of  $X$  for  $\alpha > 0.5$  must be larger than the value of  $X$  for  $\alpha = 0.5$ . Evaluating the latter one obtains

$$\begin{aligned} [X]_{\substack{\gamma=0.5 \\ U=U_B}} &= \left[ U_B^2 / (\alpha C\beta^2) \right] \left\{ \alpha^8 [2.5(1 + S\beta^2) S\beta^2] \right. \\ &\quad + \alpha^7 [(4/3 - C\beta^2)(16.5 - 18.75 C\beta^2 + 3C\beta^4)] \\ &\quad + \alpha^6 [S\beta^2(56 - 67.5 C\beta^2 + 18 C\beta^4)] \\ &\quad + \alpha^5 [S\beta^2(91 - 135.5 C\beta^2 + 47 C\beta^4)] \\ &\quad + \alpha^4 [S\beta^2(98 - 74.5 C\beta^2 + 1.5 C\beta^4)] \\ &\quad + \alpha^3 [S\beta^2(70 - 72.5 C\beta^2 + 7.75 C\beta^4)] \\ &\quad + \alpha^2 [S\beta^2(32 - 42.5 C\beta^2 + 10.5 C\beta^4)] \\ &\quad \left. + [S\beta^8] \right\} \quad (13) \end{aligned}$$

It is observed that the coefficient of each power of  $\alpha$  above is non-negative. Hence at  $U = U_B$ ,  $X$  is positive for  $\gamma > 1/2$ .

From (10) it is seen that  $X/U^2$  is a quadratic in  $U^2$ , i.e.

$$X/U^2 = A U^4 + B U^2 + C$$

and also that  $C$  is always positive. For small  $U$ , clearly  $X > 0$  for all  $\gamma$ . Further, for  $0.5 < \gamma < 3$  it is found that  $X > 0$  in the whole interval  $0 < U < U_B$ . It is thus concluded that if  $\gamma > 0.5$  loss of stability occurs only by buckling as the flowrate is increased from a value of zero.

It might be of interest to examine whether, at flow velocities higher than  $U_B$ , a transition to stability or flutter could occur. A numerical investigation was carried out for the following range of parameters

$$0.1 < \alpha < 10$$

$$0.5 < \gamma < 3$$

$$0 < U < 10 U_B$$

For numerous values of  $\alpha$ ,  $\beta$  and  $\gamma$  the roots of (6) were computed as  $U$  increased from zero. A typical root locus plot is shown in Fig. 2 corresponding to  $\beta = 0^\circ$ . Since any complex roots must occur as conjugate pairs, only the upper half of the plane is shown. When  $U = 0$ , the characteristic roots are all purely imaginary, and as  $U$  is increased, the roots trace out the curves shown. When  $U = 1.56$  a pair of roots coalesces on the negative real axis, and as  $U$  is further increased, they split, one moving in the positive and one in the negative real directions. Buckling first occurs with the vanishing of one root when  $U = 1.732$  and for all greater  $U$ , at least one root is positive

real. As seen in the figure, all roots are purely real after  $U = 3.12$ , and as  $U$  is increased, they monotonically increase in magnitude. Thus divergence is the only mode of loss of stability possible for  $\gamma > 0.5$ , even for  $U$  greater than  $U_B$ .

The Case  $\gamma < 0.5$

This case is more complex in that either buckling or flutter may occur first as the flowrate is increased, depending on the value of  $\beta$ .

For  $\beta = 0$ , Benjamin [5] has shown that stability will be lost first by flutter. For  $\beta = 90^\circ$ , on the other hand,

$$X = U^4[2(\alpha + 1)^7 + 2(\alpha + 1)^6] + U^2[\alpha^2(\alpha + 1)^6]$$

which is always positive, and thus is positive also in some neighborhood of  $\beta = 90^\circ$ . Since  $A_0$  can vanish for all  $\beta$  except  $\beta = 90^\circ$ , it is seen that near  $\beta = 90^\circ$  only buckling can occur. Thus as  $\beta$  increases from zero, a transition in the mode of loss of stability from flutter to buckling has to occur at some value of the angle,  $\beta^*$ .

To determine this transition angle  $\beta^*$ , and to obtain quantitative data of the critical value of  $U$  for the whole range  $0 \leq \beta < 90^\circ$ , a parametric computer study was carried out. A typical plot of  $U$  as a function of  $\beta$  for a given system ( $\alpha = 1.0$ ,  $\gamma = 0.25$ ) is shown in Fig. 3. In this case  $\beta^* = 26^\circ$ . In region I there are two pairs of complex conjugate roots, one of which has positive real parts. Hence in this region, loss of stability occurs by flutter. In region II there are a pair of flutter roots and two real roots, one of which is positive. Hence in this region the system experiences loss of stability by oscillation

with increasing amplitude superimposed upon a monotonic motion away from the equilibrium position. In region III the characteristic roots are all real, with at least one being positive. Hence this is a region of divergence.

A typical root locus plot for  $\beta = 0^\circ$  is presented in Fig. 4. As before only the upper half of the plane is shown. As in the case  $\gamma > 0.5$ , once all the roots become real, they monotonically increase in magnitude. Hence there are no new instability regions above the buckling region in Fig. 3. For all  $\beta > \beta^*$ , the typical root locus is the same as that shown in Fig. 2 for the case  $\gamma > 0.5$ .

A composite plot of the dependence of  $\beta^*$  on  $\gamma$  and  $\alpha$  is presented in Fig. 5. For any given physical configuration (i.e. specified values of  $\alpha$ ,  $\beta$  and  $\gamma$ ), one can determine first the mode of loss of stability. Next, the corresponding critical flowrate can be calculated from either (10) or (11). It is noted that as  $\gamma \rightarrow 0.5$ ,  $\beta^* \rightarrow 0$  independent of  $\alpha$ , which is consistent with the results of the case  $\gamma > 0.5$ .

## 5. Experiments

An overall view of the experimental set-up is given in Fig. 6. The tube segments were of thin metal (copper and brass) in commercially available standard gauges, and were of equal lengths.

The joints consisted of ball bearings and light brackets made of plexiglas. The pipes were connected across the joints by short segments of latex surgical tubing (Kent Latex Products, 0.25 inch ID, Thin Wall).

Water was used as the fluid, and its velocity was measured by means of a precision flowmeter of the rotameter type.

The additional masses of the hinges, while small, were not negligible. Further, it was found that the surgical tubing gave rise to small restoring and damping forces. A schematic of the apparatus is shown in Fig. 7. The quantities needed in the governing equations can be identified as

$$M_A = m + 2m_H$$

$$M_B = m + m_H$$

$$L_A = l + 2c$$

$$L_B = l + c$$

$$M_A a = (m + 2m_H)(0.5l + c)$$

$$M_B b = m(0.5l + c) + m_H d$$

$$I_{zz}^A = \frac{m\ell^2}{12} + m(0.5l + c)^2 + 2\bar{I}_H + m_H d^2 + m_H(l + 2c - d)^2$$

$$\bar{I}_{11}^B + M_B b^2 = \frac{m\ell^2}{12} + m(0.5l + c)^2 + \bar{I}_H + m_H d^2$$

where

$m$  = mass of each metal tube

$l$  = length of each metal tube

$m_H$  = mass of each hinge

$\bar{I}_H = I_{11}$  of each hinge with respect to its centroid.

It was suspected that the restoring and damping forces would be sensitive to the water pressure in the surgical tubing at the joints. The values of the restoring and damping constants were obtained by conducting a separate test with just the upper tube and upper hinge. The tube was closed at its lower end and pressurized with air. It was then photographed with a motion picture camera as it oscillated freely and damped out. This was repeated for several different pressures. From the observations the restoring and damping constants could be obtained in a standard fashion.

To utilize this information it was necessary to know the fluid pressure in the surgical tubing as a function of flowrate. This was obtained by assembling the pipes and hinges in the test configuration (as in Fig. 6) and replacing one joint at a time by a short tube tapped to place a pressure gauge. Then water was forced through and pressure readings could be taken. This procedure neglects the effects of expansion of the surgical tubing and of motion of the joints with increase in pressure. For small motions, however, the latter should have little effect, and the final tests were discontinued when the expansion of surgical tubing became excessive.

The results of the above preliminary tests indicated that the lower spring constant,  $K_2$ , was nearly independent of the flowrate over the range involved, while the upper spring constant,  $K_1$ , was fairly sensitive to the flowrate, as shown in Fig. 8. This could have been expected, since most of the pressure drop involved would take place at the upper joint where the flow channel was constricted down to the inside diameter of the pipe. It was also found that the damping coefficients

were nearly independent of pressure, and thus the damping is primarily due to the friction in the ball bearings.

The actual experiments to determine the instability mode behavior were performed on two different pairs of tubes, one with  $\gamma = 0.328$  and one with  $\gamma = 1.09$ . The dimensions of the two sets of pipes and of the hinges are shown in the table below. The same hinges were used with each set of tubes.

	Set I $\gamma = 0.328$	Set II $\gamma = 1.09$
Type	Copper 1/4"OD x .035 wall	Brass 5/16"OD x .015 wall
m (slugs)	0.000198	0.000123
$m_H$ (slugs)	0.000059	0.000059
$l$ (inch)	12.0	12.0
A (sq. inch)	0.0254	0.0625
$K_2$ (in-lb)	0.206	0.206
$R_1, R_2$ (in-lb-sec)	0.030	0.030
c (inch)	0.750	0.750
d (inch)	1.295	1.295
$\bar{I}_H$ (in <sup>2</sup> -slug)	0.000135	0.000135

With these values, the coefficients in the governing equations were evaluated and the critical flowrates obtained as described in the first part of the paper. The results are shown in Figs. 9 and 10. The solid curves denote the theoretical predictions.

The tests were performed quasi-statically. Thus the flowrate was increased in small increments, and at each step the two pipes were manually displaced two degrees from the vertical and released with no

initial velocity. This was repeated until a flowrate was reached at which the resulting motion did not subside. The onset of flutter was marked by steady periodic oscillations. Upon slightly increasing the flowrate, there resulted oscillations with increasing amplitude.

In certain cases, the onset of buckling was somewhat difficult to determine precisely. This was due to unavoidable small eccentricities in the system which caused the position of equilibrium to change slightly with an increase in flowrate. As a result, the onset of buckling was evidenced by large deflections corresponding to a finite (but narrow) range of flowrates. In the majority of cases, however, as the flowrate was increased in small steps, the transition to the buckled state occurred quite suddenly. The associated deflections were so large as to require stops to prevent the system from being damaged. Thus in most cases an unambiguous buckling load could be determined. The above procedure was repeated for each increasing value of  $\beta$ . The range of the data taken was limited by the expansion of the surgical tubing at large flowrates.

The tubing gave rise to another problem. As it is manufactured and packed, it has a slight permanent curvature. When the pipes and joints were assembled, the surgical tubing was arranged such that the plane of motion of the joint was normal to the plane of curvature of the tubing. Without this precaution the two metal tubes could not be aligned even in the absence of flow. Thus, when  $\beta$  was changed, it was also necessary to rearrange the surgical tubing. And in doing this great care had to be taken to ascertain that the tubing was not stretched. It was found early in the experimentation that even a small amount of stretching resulted in considerable changes in the buckling loads.

The surgical tubing also gave rise to a notable non-linear effect. When stability was lost by flutter it was found that an increase of the initial displacement resulted in a lower critical flow-rate. This implies the existence of either non-linear restoring or damping forces of the "softening" type and, in fact, it was found from the dynamic amplitude-time data (used to determine the spring constants) that non-linear damping was the predominant factor. In the case of such "softening" type forces one cannot invoke the theorem due to Lyapunov as in [3], which asserts that the instability threshold for a non-linear system is the same as that for the corresponding linearized system. Work is underway to evaluate this effect in a quantitative way, but until then this does serve to emphasize the need for employing uniform, small initial conditions in tests of this type.

The results of the tests are summarized in Figs. 9 and 10. For  $\gamma = 0.328$ , the transition angle  $\beta^*$  at which the initial instability changed from flutter to buckling was predicted analytically to lie between  $21^\circ$  and  $22^\circ$ . In the test, the pin angle  $\beta$  was increased in  $5^\circ$  increments and as seen in Fig. 10 the changeover occurred between  $\beta = 20^\circ$  and  $\beta = 25^\circ$ . No closer determination was attempted, since the inaccuracies in the values of the spring and damping constants rendered any further refinement meaningless. The transition angle provides a measure of the correlation between the experimental system and the idealized one considered in the first portion of the paper. For the latter, with  $\gamma = 0.328$ , Fig. 5 predicts a transition angle of  $20^\circ$  and this agrees well with the transition angle for the experimental system, which was predicted as  $21^\circ < \beta^* < 22^\circ$  and measured as  $20^\circ < \beta^* < 25^\circ$ .

In each of the cases, the measured buckling loads were lower than those predicted, as would be expected due to the unavoidable presence of small eccentricities. The agreement in each case tends to fall off as  $\beta$  is increased. For the flutter case ( $\gamma = 0.328$ ) the discrepancy varied from 4% at  $\beta = 0^\circ$  to 10% at  $\beta = 40^\circ$ . In the buckling case ( $\gamma = 1.09$ ) the discrepancy varied from 8% at  $\beta = 0^\circ$  to 18% at  $\beta = 40^\circ$ . The increasing discrepancy as  $\beta$  is increased is probably attributable to the normal forces applied to the bearing which are present in increasing magnitude as  $\beta$  is increased. This would tend to accentuate any eccentricities in the joint and further cause beam-type bending in the tubes themselves, giving rise to further misalignment. In view of the unavoidable imperfections present in any mechanical system used to study buckling behavior, the agreement between the theory and the experiment obtained herein is considered to be acceptable.

#### 5. Concluding Remarks

By considering a spatial system of articulated pipes, it has been shown that the various types of loss of stability, characteristic of idealized non-conservative systems, can in fact be obtained in a physically realizable model. It has also been verified that the assumption of one-dimensional flow and the use of linearized equations of motion are adequate to determine the boundaries of the various regions of instability.

However, an important aspect of such systems has been observed, which must undoubtedly be considered in applying the above-mentioned

assumptions to stability problems in pipes conveying fluid. As found in the experimentation, the softening-type non-linear behavior of the flexible joints will significantly change the stability characteristics of the system. Thus a careful characterization of the non-linear behavior of coupling tubes is a necessary prerequisite to the practical stability analysis of such devices as fluid-driven control systems.

#### REFERENCES

- [1] Bolotin, V. V., Nonconservative Problems of the Theory of Elastic Stability, Moscow, 1961; English translation published by Pergamon Press, New York, 1963.
- [2] Herrmann, G., "Stability of Equilibrium of Elastic Systems Subjected to Nonconservative Forces," Applied Mechanics Reviews, Vol. 20, 1967, pp. 103-108.
- [3] Ziegler, H., Principles of Elastic Stability, Blaisdell Publishing Company, Waltham, Massachusetts, 1968.
- [4] Herrmann, G., "Dynamics and Stability of Mechanical Systems with Follower Forces," NASA Contractor Report CR-1782, November 1971.
- [5] Benjamin, T.B., "Dynamics of a System of Articulated Pipes Conveying Fluid," Parts 1 and 2, Proc. Royal Soc. A, Vol. 261, pp. 457-499, 1961.

LIST OF ILLUSTRATIONS

- Figure 1. The System of Articulated Pipes
- Figure 2. Typical Root Locus for  $\gamma > 1/2$
- Figure 3. Typical Flowrate  $U$  vs. Pin Angle  $\beta$  for  $\gamma < 1/2$
- Figure 4. Typical Root Locus for  $\gamma < 1/2$
- Figure 5. Locus of Transition Angle  $\beta^*$  vs. Mass Ratio  $\gamma$
- Figure 6. The Experimental System
- Figure 7. Schematic of the Experimental System
- Figure 8. Spring Constant  $K_1$  vs. Flowrate  $U$
- Figure 9. Theoretical and Experimental Results for  $\gamma = 1.09$
- Figure 10. Theoretical and Experimental Results for  $\gamma = 0.328$

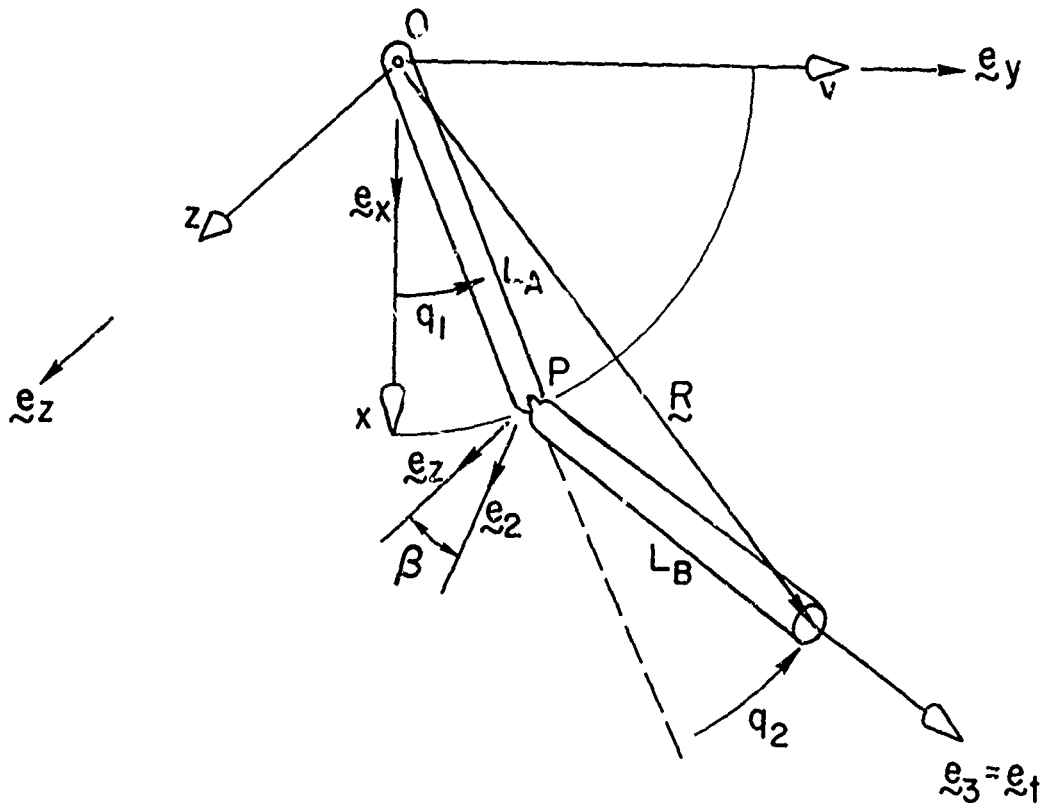
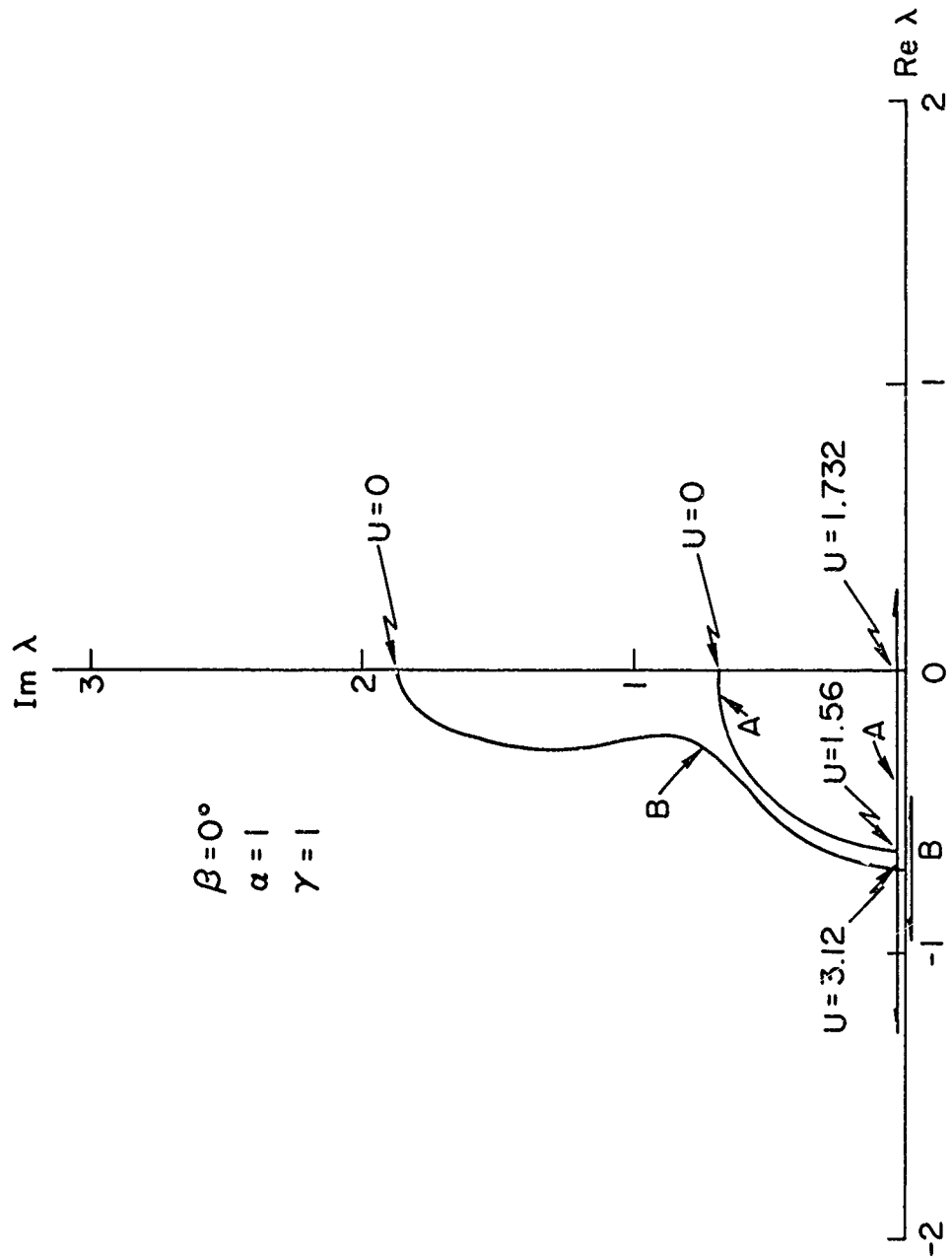


Figure 1. The System of Articulated Pipes



$\beta = 0^\circ$   
 $\alpha = 1$   
 $\gamma = 1$

Figure 2. Typical Root Locus for  $\gamma > 1/2$

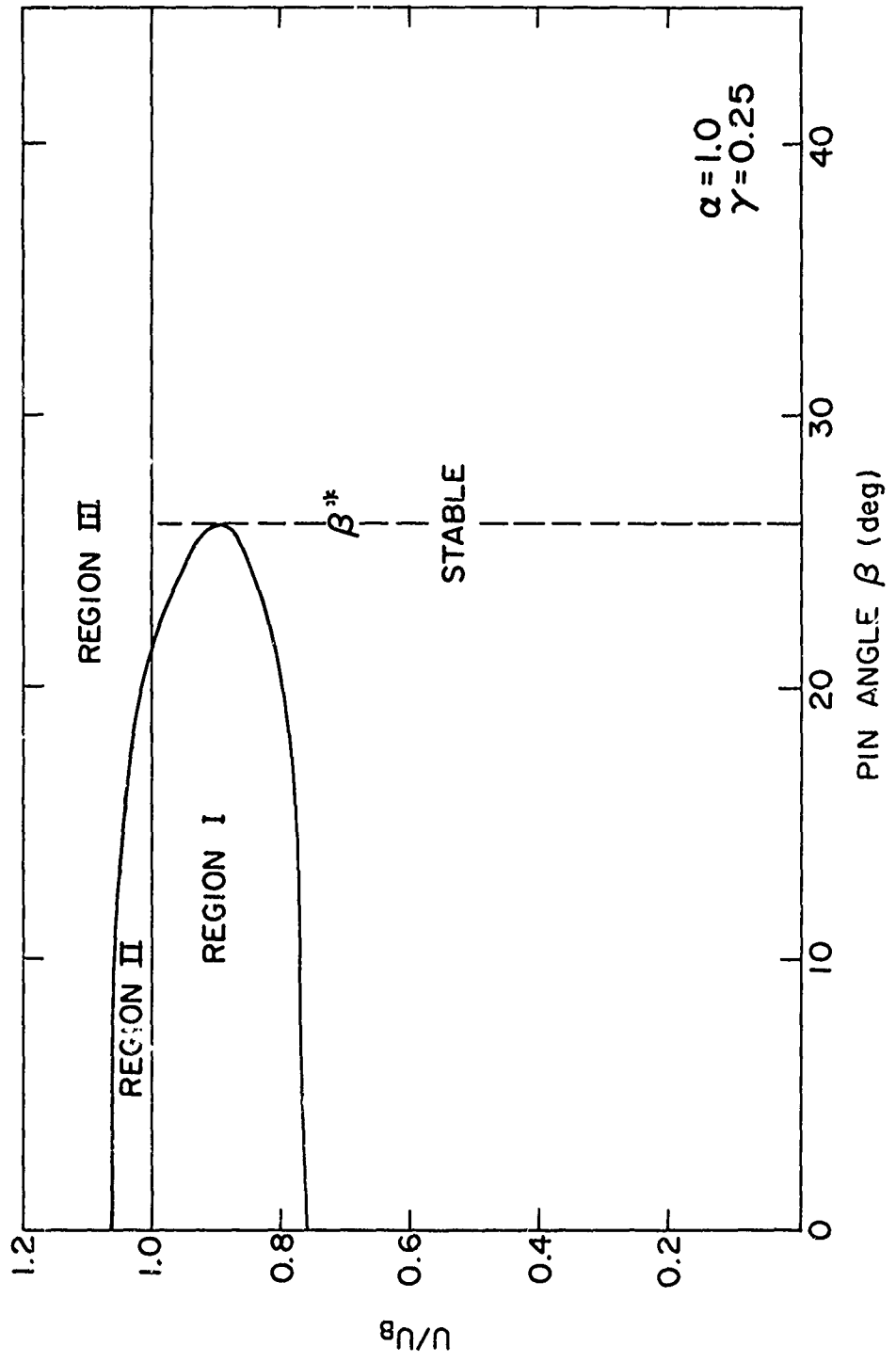


Figure 3. Typical Flowrate  $U$  vs. Pin Angle  $\beta$  for  $\gamma < 1/2$



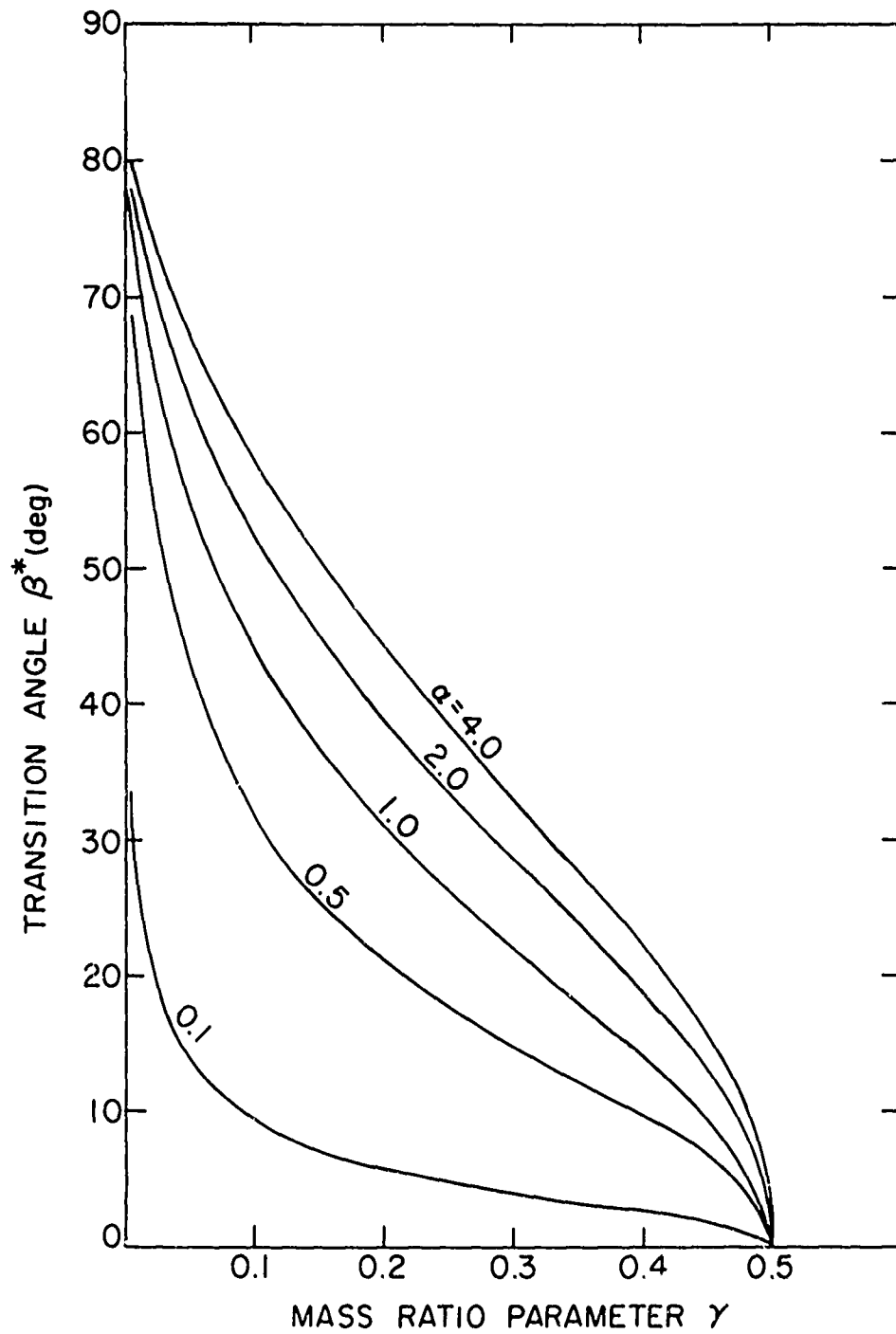


Figure 5. Locus of Transition Angle  $\beta^*$  vs. Mass Ratio  $\gamma$

Reproduced from  
best available copy.

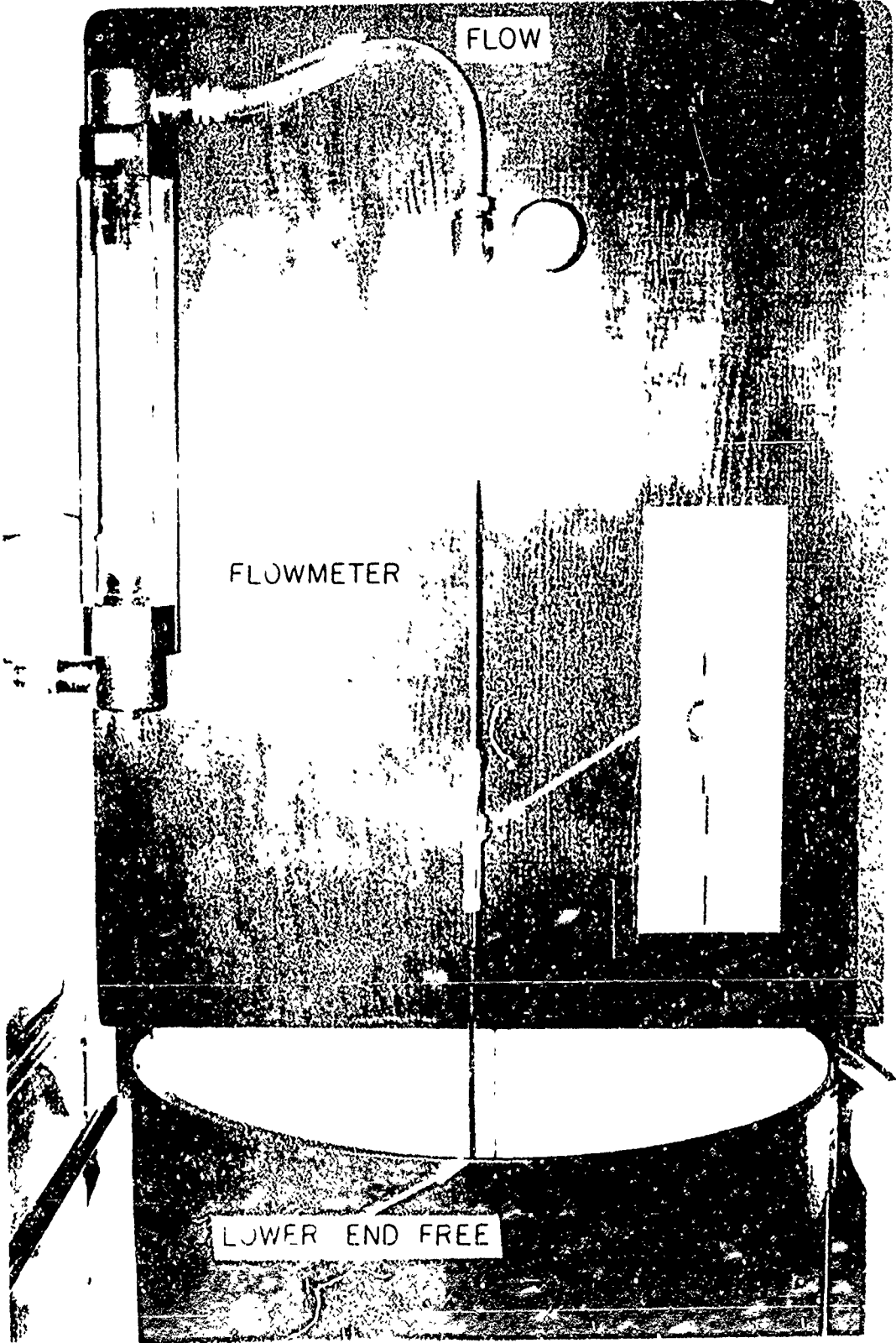


Figure 1. The experimental system.

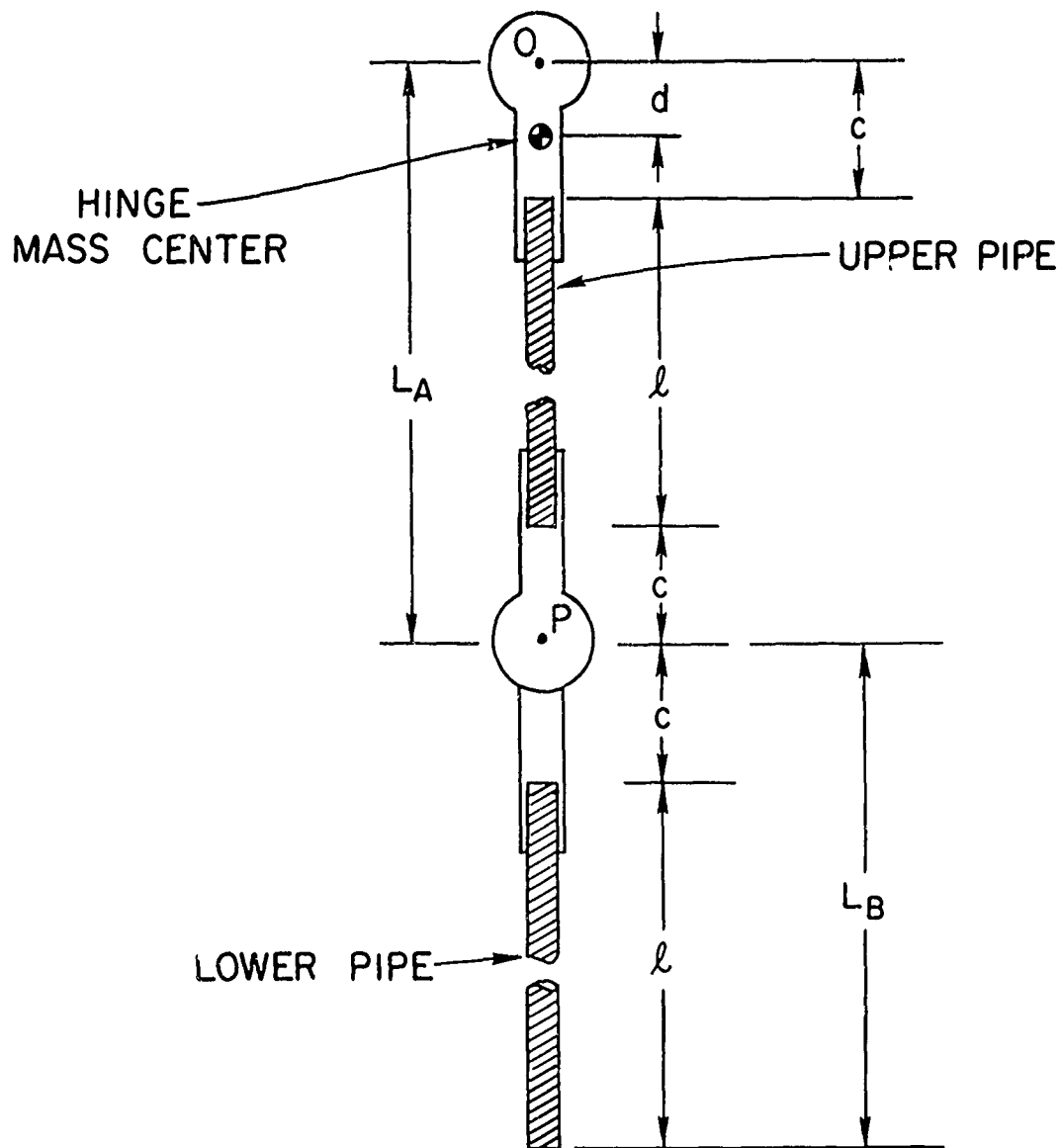


Figure 7. Schematic of the Experimental System

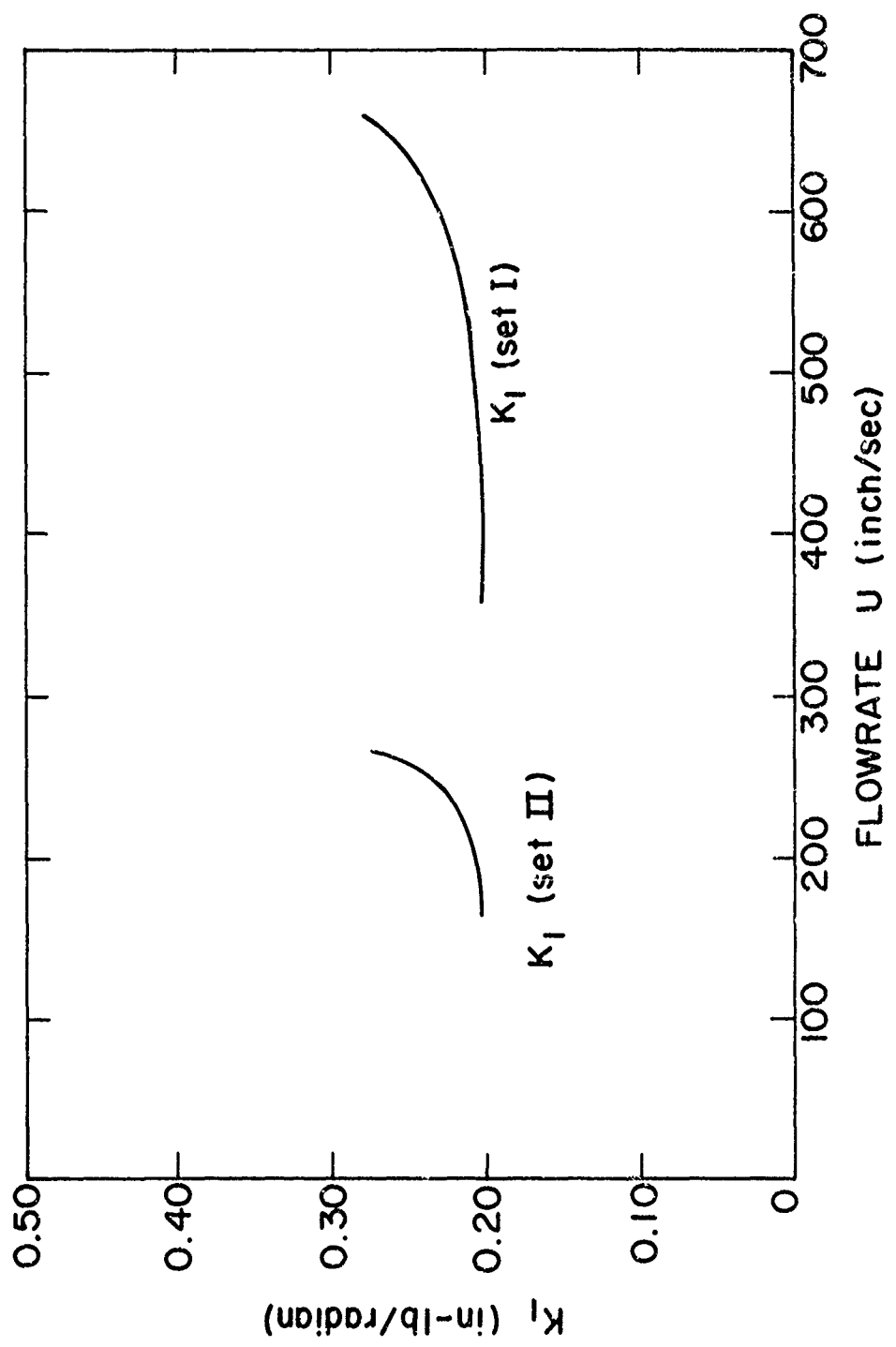


Figure 8. Spring Constant  $K_I$  vs. Flowrate  $U$

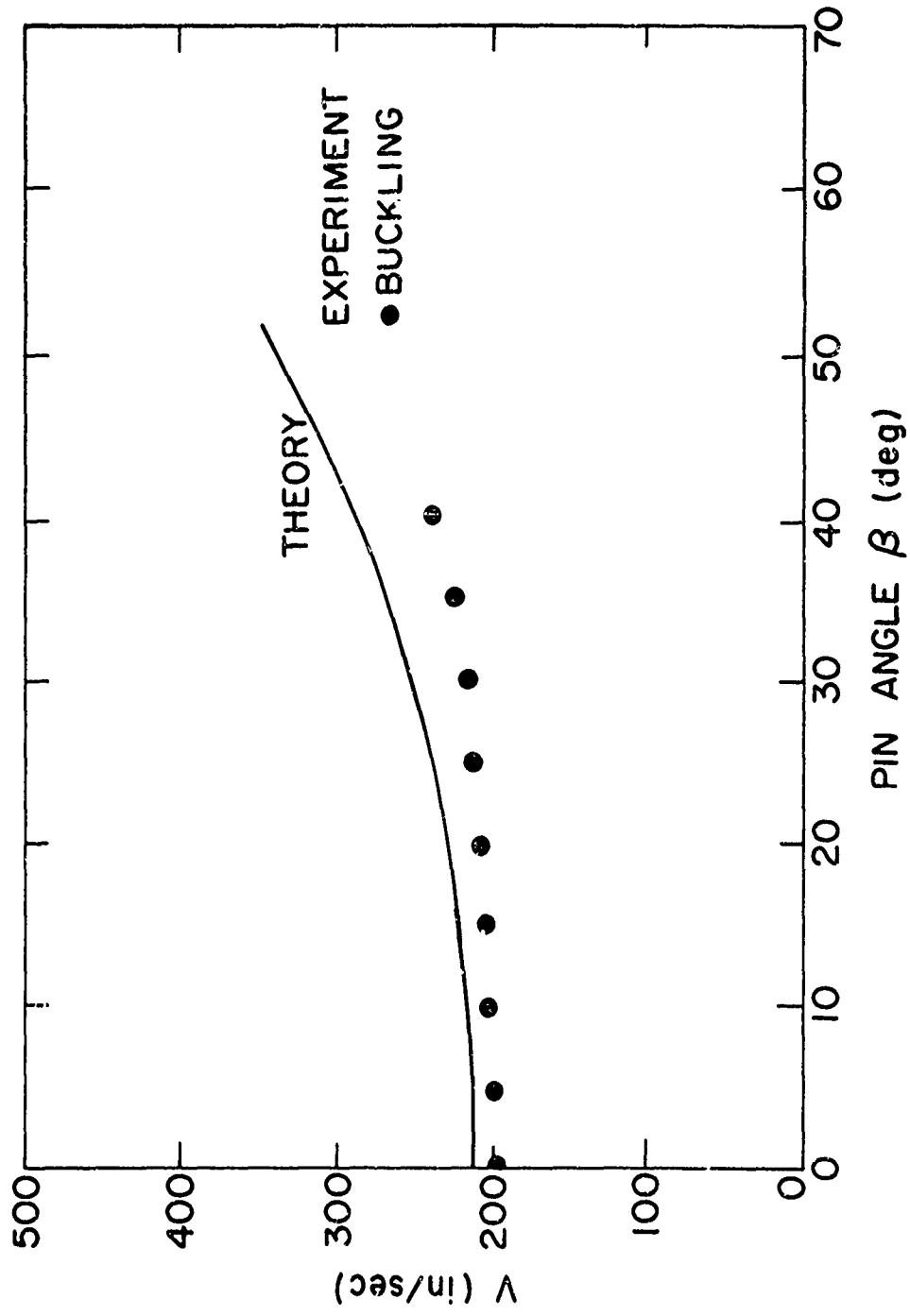


Figure 9. Theoretical and Experimental Results for  $\gamma = 1.09$

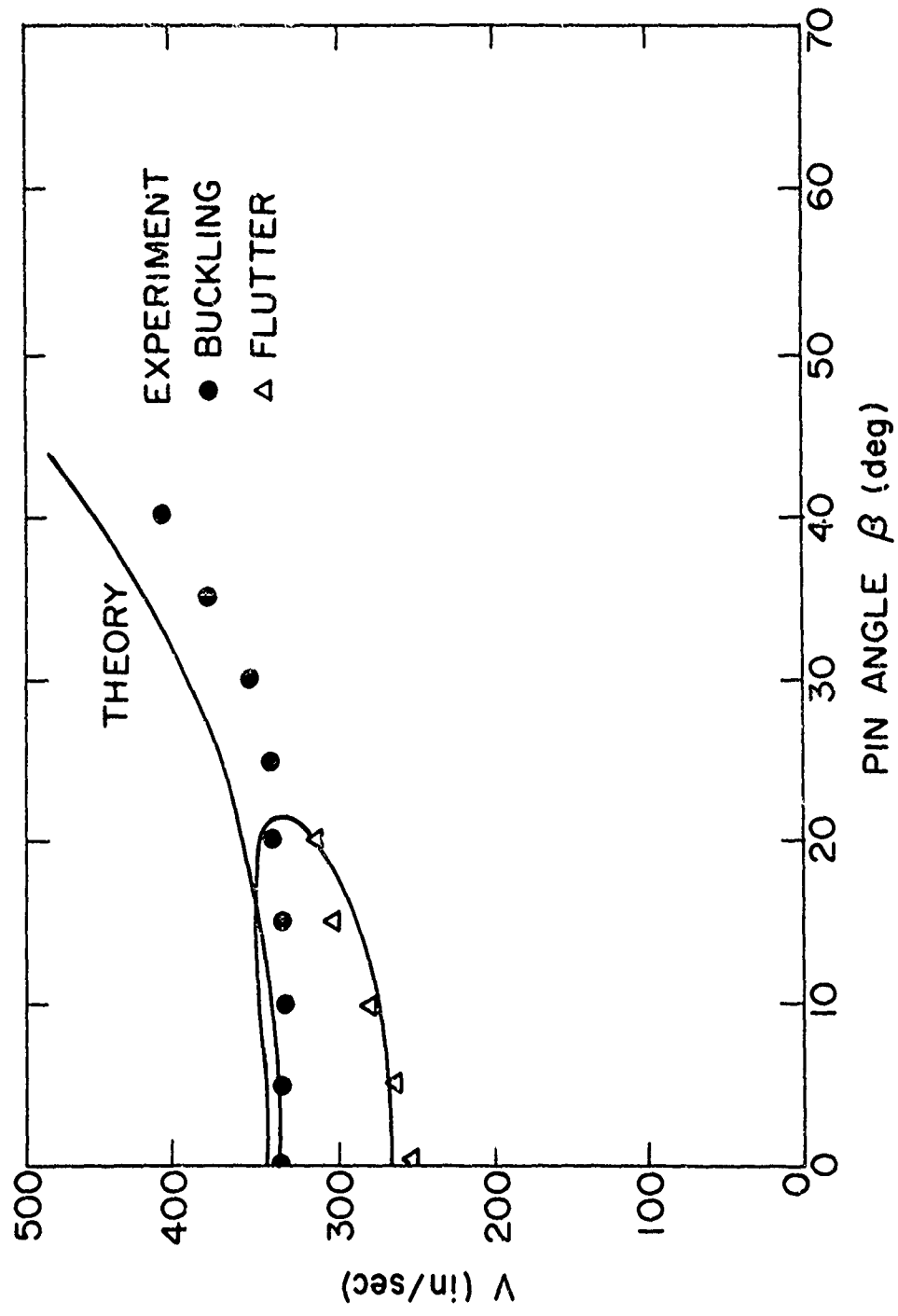


Figure 10. Theoretical and Experimental Results for  $\gamma = 0.328$